01 Apr 1991

Vapor-Liquid Equilibrium Data For The NH3-H2O System And Its Description With A Modified Cubic Equation Of State

Thomas M. Smolen

David B. Manley
Missouri University of Science and Technology

Bruce E. Poling
Missouri University of Science and Technology, bruce.poling@utoledo.edu

Recommended Citation

T. M. Smolen et al., "Vapor-Liquid Equilibrium Data For The NH3-H2O System And Its Description With A Modified Cubic Equation Of State," *Journal of Chemical and Engineering Data*, vol. 36, no. 2, pp. 202 - 208, American Chemical Society, Apr 1991.
The definitive version is available at https://doi.org/10.1021/je00002a017

investigation, 0.1029 ± 0.0007 V. Furthermore, the newer set of emf data of Merken et al. (7) leads to a value of 0.103 19 ± 0.000 05 V. One may conclude that the discrepancy resides in the experimental measurements, rather than, as postulated by Merken et al. (11), in the failure of Sadek et al. to allow for ion pairing and their use of too low a value for the dielectric constant.

As expected, the transfer properties given in Table VI reflect the decreasing stabilization of HCl as water is replaced by the organic solvent. An increase of pK_2 as 2-methoxyethanol is added to the water solvent is evident in Table VII. Here, changes in the ion-solvent interaction pattern are presumably reinforced by enhanced ion-ion interaction favored by the decreasing dielectric constant of the medium.

Registry No. AgCl, 7783-90-6; Ag, 7440-22-4; HCl, 7647-01-0; H_2, 1333-74-0; PO_4^{3-}, 14265-44-2; $H_2PO_4^-$, 14066-20-7; KH_2PO_4, 7778-77-0; Na_2HPO_4, 7558-79-4; 2-methoxyethanol, 109-86-4.

Literature Cited

(1) Taylor, M. J.; Walter, C. A.; Elford, B. C. *Cryobiology* **1978**, *15*, 452.
(2) Taylor, M. J.; Pignat, Y. *Cryobiology* **1982**, *19*, 99.
(3) Vega, C. A.; Rosado, E.; Bates, R. G. *J. Chem. Eng. Data* **1990**, *35*, 407.
(4) Vega, C. A.; Delgado, S. *J. Chem. Eng. Data* **1986**, *31*, 74.
(5) Thun, H. P.; Staples, B. R.; Bates, R. G. *J. Res. Natl. Bur. Stand., Sect. A.* **1970**, *74*, 641.
(6) Sadek, H.; Tadros, T. F.; El-Harakany, A. A. *Electrochim. Acta* **1971**, *16*, 339.
(7) Merken, G. V.; Thun, H. P.; Verbeek, F. *Bull. Soc. Chim. Belg.* **1977**, *86*, 649.
(8) Shanbhag, P. M.; Vega, C. A.; Bates, R. G. *Bull. Soc. Chim. Belg.* **1981**, *90*, 1.
(9) Simon, W.; Mörikofer, A.; Heilbronner, E. *Helv. Chim. Acta* **1957**, *40*, 1918. Simon, W. Thesis, E. T. H., Juris-Verlag, Zurich, 1956.
(10) Bates, R. G. *Determination of pH, Theory and Practice*, *2nd* ed.; Wiley: New York, 1973; Chapter 10, pp 248-9.
(11) DeRossi, C.; Sesta, B.; Battistini, M.; Petrucci, S. *J. Am. Chem. Soc.* **1972**, *94*, 2961.
(12) Vega, C. A.; Rosado, E.; Bates, R. G. *J. Chem. Thermodyn.*, in press.
(13) Merken, G. V.; Thun, H. P.; Verbeek, F. *Electrochim. Acta* **1974**, *19*, 947.
(14) Merken, G. V.; Thun, H. P.; Verbeek, F. *Electrochim. Acta* **1976**, *21*, 11.
(15) Klein, S. D.; Bates, R. G. *Bull. Soc. Chim. Belg.* **1981**, *90*, 123.
(16) Bates, R. G.; Bower, V. E. *J. Res. Natl. Bur. Stand.* **1954**, *53*, 283.
(17) Bates, R. G.; Acree, S. F. *J. Res. Natl. Bur. Stand.* **1943**, *30*, 129.

Received for review May 24, 1990. Accepted September 24, 1990.

Vapor–Liquid Equilibrium Data for the NH_3–H_2O System and Its Description with a Modified Cubic Equation of State

Thomas M. Smolen, David B. Manley, and Bruce E. Poling*

Departments of Chemical Engineering, University of Missouri—Rolla, Rolla, Missouri 65401, and University of Toledo, Toledo, Ohio 43606

New pressure–temperature–overall composition vapor–liquid equilibrium (VLE) data are reported for the ammonia–water system at five temperatures between 20 and 140 °C and up to 500 psia. These data have been converted to *T–P–x* data, and vapor-phase compositions have been calculated by means of a Redlich–Kwong equation of state modified to include Peneloux's volume translation and a density-dependent mixing rule. In order to achieve agreement of calculated vapor-phase compositions with previous literature results, it was necessary to use different k_{ij} values in the vapor and liquid phases.

Introduction

There have been a number of experimental (*1–9*) and computational (*1*, *10–14*) efforts to characterize the vapor–liquid equilibrium (VLE) behavior of the NH_3–H_2O system. Gillespie et al. (*1*) point out that, prior to their work, there was disagreement between experimental and calculated vapor-phase compositions, especially at high ammonia concentrations. Some authors had attributed these discrepancies to thermodynamically inconsistent data (Edwards et al. (*14*), for example), others to shortcomings in existing models (Peng and Robinson (*12*) and Heidemann and Rizvi (*11*), for example). Gillespie et al. (*1*) were able to resolve this disagreement. They first took an extensive data set that included both total pressure and *T–P–x–y* data and then fit these data with an activity coefficient based model with three parameters for the liquid phase and an equation of state with an adjustable cross-virial coefficient for the vapor phase.

The objectives of the work described herein were three-fold. The first objective was to measure a set of pressure–total composition data that was more precise than those sets in the literature. This had already been done in our laboratory for other systems. The second objective was to correlate these data with an equation of state that included recent improvements in equation-of-state techniques. The third objective was to see if the improved accuracy of our *T–P–x* data and the improved equation of state methods could successfully remove discrepancies in the vapor-phase compositions, as Gillespie et al. (*1*) had done with their *T–P–x–y* data and activity coefficient model.

Experimental Section

Total composition–pressure–temperature data were determined at the nominal temperatures of 20, 50, 80, 110, and 140 °C and up to 500 psia. At the lowest three temperatures, the data covered the entire composition range, but the pressure limitation did not allow data to be taken over the entire range at the highest two temperatures. The VLE was established in cells that are shown in Figure 1. These cells, which are described in more detail in ref 15, consist of a sample compartment, a stainless steel diaphragm, and a transducer. Pressure was measured by adjusting the nitrogen pressure in the upper chamber of the cell until the diaphragm was forced into its null position, which was sensed by the transducer. The nitrogen pressure was measured with one of three digital pressure gauges, which had ranges of 0–20, 0–150, and 0–2500 psig

* To whom correspondence should be addressed at the University of Toledo.

0021-9568/91/1736-0202$02.50/0

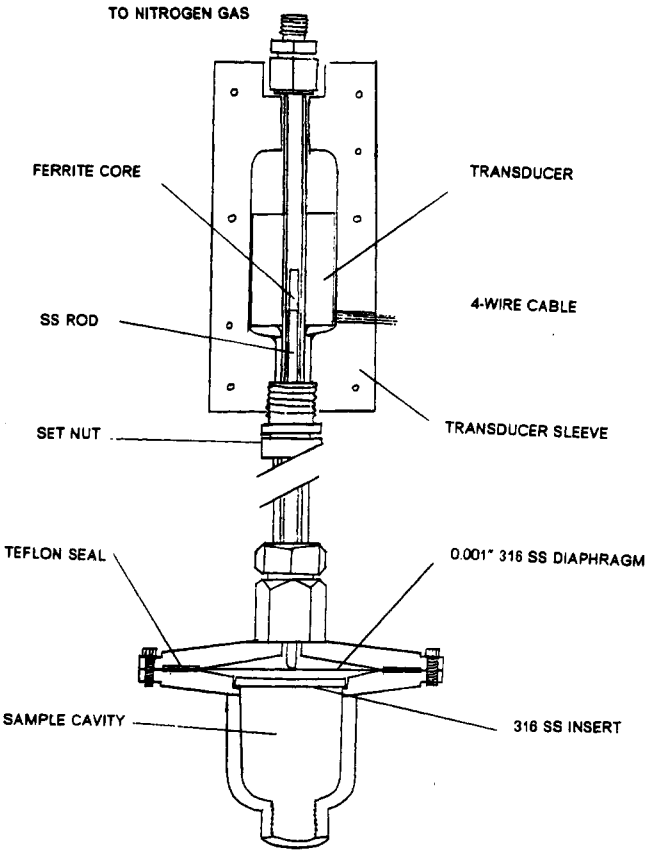

Figure 1. Vapor–liquid equilibrium cell.

Table I. Values of a, b, and c Used in Equation 3 for Ammonia

T, K	a, bar cm^6 mol^{-2}	b, cm^3 mol^{-1}	c, cm^3 mol^{-1}
293.15	7030829	13.305	21.895
323.15	5926434	13.273	17.757
353.15	5144642	12.524	15.638
383.15	4531602	10.740	15.169
413.15	3930000	8.15	15.0

and were accurate to 0.008, 0.06, and 1 psia, respectively. The estimated uncertainties in the pressure due to uncertainties in all variables were ±0.05 psia for $P < 20$ psia, ±0.5 psia for $P < 150$ psia, and ±2 psia for $P > 150$ psia. Temperature was measured with an Azonix digital thermometer, which was accurate to 0.01 °C. Total compositions were determined from the masses of the components, which were measured to the nearest milligram with an estimated accuracy of ±0.001 g.

Ammonia was loaded into an evacuated 300-cm^3 stainless steel cylinder, degassed by a series of freeze–thaw cycles with liquid nitrogen, and stored for future loading into the VLE cells. Gas chromatographic analysis with a thermal conductivity detector indicated an NH_3 purity of at least 99.99%. Water was deionized, distilled in a stainless steel still, and boiled for 20 min to remove dissolved gases. A stainless steel cylinder was then completely filled with the boiling hot water that was later used to fill the VLE cells. Finally, the VLE cells were charged by means of a manifold, details of which can be found in ref 15.

The experimental procedure consisted of loading three VLE cells with a desired composition and then measuring pressures and temperatures through the cycle of 20 °C up to the maximum temperature and then back to 20 °C. This procedure allowed detection of leaks and/or corrosion, both of which occasionally occurred, and also ensured that equilibrium was attained in the cells. Corrosion was minimized by means of a passivation technique described in ref 16.

Table II. Values of a, b, and c Used in Equation 3 for Water

T, K	a, bar cm^6 mol^{-2}	b, cm^3 mol^{-1}	c, cm^3 mol^{-1}
293.15	30657320	6.889	68.563
323.15	22042290	8.447	47.621
353.15	16924170	9.429	35.033
383.15	13605380	10.110	26.764
413.15	11354300	10.560	21.187

Equation of State

Equations that were used to calculate the compositions of the liquid and vapor phases from the experimental data included a volume balance

$$L = \frac{V^v - V_{cell}/N_{tot}}{V^v - V^l} \tag{1}$$

a material balance equation for each component

$$x_i = \frac{z_i}{L + K_i(1 - L)} \tag{2}$$

and the equation of state

$$P = \frac{RT}{V - b} - \frac{a}{(V + c)(V + b + 2c)} \tag{3}$$

where

$$a = \sum_i \sum_j x_i x_j \left((a_i a_j)^{1/2}(1 - k_{ij}) + \frac{b}{VRT}(x_i \lambda_{ij} + x_j \lambda_{ji}) \right) \tag{4}$$

$$b = \sum_i x_i b_i \tag{5}$$

and

$$c = \sum_i x_i c_i \tag{6}$$

Equation 3 is the Redlich–Kwong equation of state modified by inclusion of a volume translation parameter, c, as described by Peneloux et al. (*17*). The three-parameter equation was chosen because it can reproduce exactly the vapor pressure, saturated liquid volume, and saturated vapor volume of the pure components at a particular temperature. In fact, the final procedure used to set the pure-component parameters a–c was slightly modified from this approach. For ammonia at the lowest four temperatures, a–c were set with the vapor pressure, saturated liquid volume, and the fugacity coefficient of the saturated vapor. At the highest temperature, 413.15 K, which is above the critical temperature for ammonia, the three constants were set by fitting volumes along the isotherm up to pressures of 130 bar. Pure ammonia properties were taken from refs 18 and 19, and the values of a–c are given in Table I. For water, the vapor pressure was sufficiently low that deviations from ideal gas behavior were not large enough to effectively set a third parameter in the equation of state. Thus, the three constants were set with four conditions: the vapor pressure, the saturated liquid volume, the saturated vapor volume, and the second virial coefficient, B, which is related to the equation of state constants by

$$B = b - c - a/RT \tag{7}$$

Water properties were taken from refs 20 and 21, and the a–b–c values are shown in Table II.

Equation 4 is a density-dependent mixing rule and was first presented by Panagiotopoulous and Reid (*22*). This mixing rule allows the introduction of the additional parameters λ_{ij} and λ_{ji}. Panagiotopoulous and Reid (*22*) used the condition that $\lambda_{ij} = -\lambda_{ji}$ so that there were two adjustable parameters for each binary pair. In this study, this condition was not used, and λ_{12} and λ_{21} were allowed to vary independently. When λ_{12}, λ_{21},

Table III. Parameter Values for Equation 4[a]

T, K	k_{ij}^v	k_{ij}^l	λ_{12}, bar^2 cm^9/mol^3 × 10^{-10}
293.15	−1.3	−0.178	−21.17
323.15	−1.06	−0.113	−3.71
353.15	−0.82	−0.058	7.96
383.15	−0.58	−0.009	17.91
413.15	−0.34	0.0363	26.08

[a] NH_3 is component 1.

Table IV. Compositioins and Experimental Pressures at 293.15 K

z_{H_2O}	x_{H_2O}	y_{H_2O}	P_{exp}, psia
0.9517	0.9518	0.351	0.920
0.9517	0.9518	0.351	0.922
0.9478	0.9479	0.329	0.952
0.9478	0.9479	0.329	0.968
0.9283	0.9284	0.246	1.236
0.9028	0.9030	0.174	1.686
0.8956	0.8958	0.159	1.813
0.8506	0.8508	0.0941	2.754
0.8506	0.8508	0.0941	2.814
0.8500	0.8503	0.0936	2.796
0.8500	0.8503	0.0936	2.824
0.8396	0.8399	0.0834	3.064
0.8396	0.8399	0.0834	3.116
0.8001	0.8004	0.0548	4.257
0.8001	0.8004	0.0548	4.276
0.7976	0.7979	0.0534	4.420
0.7975	0.7979	0.0534	4.418
0.7975	0.7979	0.0534	4.551
0.7455	0.7456	0.0313	6.805
0.7455	0.7456	0.0313	6.806
0.6990	0.6992	0.0198	9.674
0.6980	0.6981	0.0196	9.855
0.6980	0.6981	0.0196	9.838
0.6014	0.6019	0.007 83	19.394
0.6014	0.6019	0.007 83	19.396
0.5927	0.5933	0.007 22	20.593
0.5927	0.5933	0.007 22	20.591
0.5916	0.5922	0.007 15	20.443
0.5916	0.5922	0.007 15	20.432
0.4985	0.4995	0.003 09	36.170
0.4985	0.4995	0.003 09	36.082
0.4973	0.4985	0.003 06	36.395
0.4973	0.4985	0.003 06	36.261
0.2992	0.3016	0.000 624	77.510
0.2992	0.3016	0.000 624	77.512
0.2972	0.2999	0.000 617	77.829
0.2972	0.2999	0.000 617	77.979
0.2074	0.2088	0.000 323	96.158
0.2074	0.2088	0.000 323	96.150
0.2074	0.2089	0.000 324	96.028
0.2074	0.2089	0.000 324	96.038
0.1071	0.1083	0.000 155	109.317
0.1071	0.1083	0.000 155	109.292
0.0996	0.1006	0.000 145	110.416
0.0996	0.1006	0.000 145	110.391
0.0990	0.1000	0.000 144	110.508
0.0990	0.1000	0.000 144	110.414
0.0582	0.0588	0.000 0916	115.970
0.0582	0.0588	0.000 0916	116.009
0.0499	0.0506	0.000 0806	117.458
0.0464	0.0466	0.000 0753	117.508
0.0464	0.0466	0.000 0753	117.434
0.0461	0.0466	0.000 0754	117.572
0.0461	0.0466	0.000 0754	117.578
0.0451	0.0457	0.000 0741	118.085
0.0395	0.0398	0.000 0659	118.417
0.0395	0.0398	0.000 0659	118.225

and k_{ij} were fit to the observed pressure behavior, it was found that λ_{21} was only a weak function of temperature, so λ_{21} was set to the value that gave the best fit, which was 27 × 10^{10} bar^2 cm^9 mol^{-3}. Next, when λ_{12} and k_{ij} were adjusted so that the equation of state matched the observed pressure behavior,

Table V. Compositions and Experimental Pressures at 323.15 K

z_{H_2O}	x_{H_2O}	y_{H_2O}	P_{exp}, psia
0.9517	0.9519	0.441	3.881
0.9517	0.9519	0.441	3.885
0.9478	0.9481	0.419	4.051
0.9478	0.9481	0.419	4.044
0.9283	0.9287	0.325	5.020
0.9028	0.9033	0.241	6.486
0.9028	0.9033	0.241	6.506
0.8956	0.8962	0.222	6.951
0.8956	0.8962	0.222	6.979
0.8506	0.8513	0.139	10.192
0.8506	0.8513	0.139	10.199
0.8500	0.8509	0.139	10.247
0.8500	0.8509	0.139	10.275
0.8396	0.8404	0.125	11.199
0.8396	0.8404	0.125	11.231
0.8001	0.8010	0.0864	15.004
0.8001	0.8010	0.0864	15.029
0.7976	0.7986	0.0845	15.449
0.7975	0.7987	0.0846	15.432
0.7975	0.7987	0.0846	15.515
0.7455	0.7457	0.0529	22.532
0.7455	0.7457	0.0529	22.532
0.6990	0.6994	0.0359	30.772
0.6980	0.6983	0.0356	31.102
0.6980	0.6983	0.0356	31.037
0.6014	0.6028	0.0168	56.173
0.6014	0.6028	0.0168	56.125
0.5927	0.5943	0.0158	59.079
0.5927	0.5943	0.0158	59.008
0.5916	0.5932	0.0157	58.713
0.5916	0.5932	0.0157	58.657
0.4985	0.5009	0.008 14	94.808
0.4985	0.5009	0.008 14	94.776
0.4973	0.5001	0.008 10	95.384
0.4973	0.5001	0.008 10	95.486
0.2992	0.3046	0.002 49	183.693
0.2992	0.3046	0.002 49	183.723
0.2972	0.3033	0.002 47	184.491
0.2972	0.3033	0.002 47	184.575
0.2074	0.2107	0.001 50	225.414
0.2074	0.2107	0.001 50	225.205
0.2074	0.2104	0.001 50	225.433
0.2074	0.2104	0.001 50	225.416
0.1071	0.1099	0.000 803	256.696
0.0996	0.1017	0.000 752	259.310
0.0990	0.1013	0.000 749	259.487
0.0582	0.0596	0.000 479	272.975
0.0499	0.0513	0.000 422	277.271
0.0464	0.0468	0.000 390	277.004
0.0464	0.0468	0.000 390	276.572
0.0461	0.0473	0.000 393	277.403
0.0451	0.0464	0.000 386	278.262
0.0395	0.0400	0.000 340	279.695
0.0395	0.0400	0.000 340	278.715

it was found that the calculated vapor-phase compositions did not match literature values. This problem was eliminated when k_{ij} was allowed to take on different values in the liquid and vapor phases. The values of k_{ij}^l, k_{ij}^v, and λ_{12} that were used are shown in Table III, and their variation with temperature is shown in Figures 2 and 3. Note that, unlike λ, k_{ij} values are symmetric, i.e., $k_{12} = k_{21}$.

Results

Quantities that were measured experimentally included temperature, pressure, mass of ammonia, mass of water, and cell volume. Equations 1–6 were used to calculate the final results, which are shown in Tables IV-VIII. Pressures in these tables have been adjusted from the experimental to the nominal temperatures of 20, 50, 80, 110, and 140 °C. The difference between the experimental and nominal temperature was never more than 0.1 °C. Values of z_i, the overall mole fractions, were calculated directly from the masses. Generally three cells

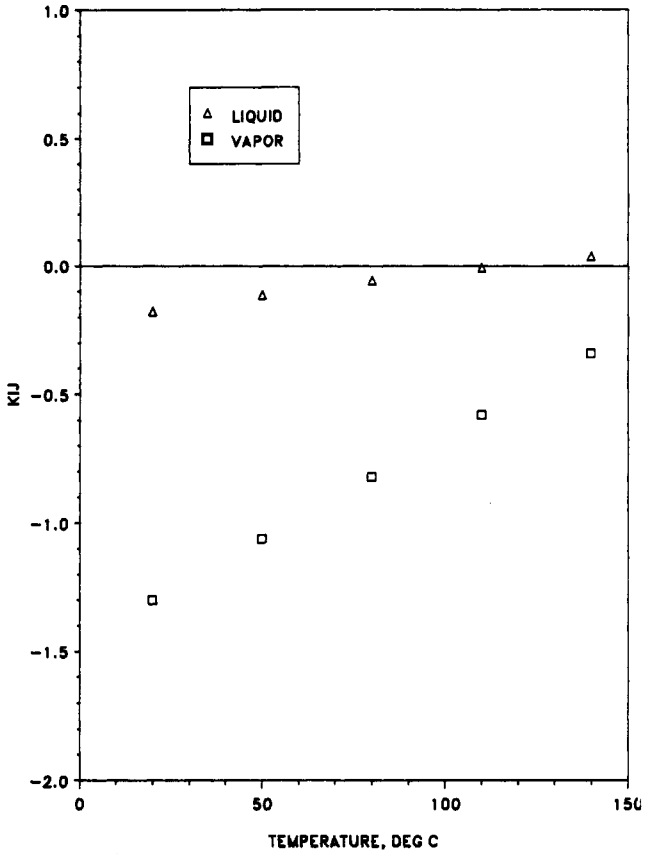

Figure 2. k_{ij}^{l} and k_{ij}^{v} versus temperature.

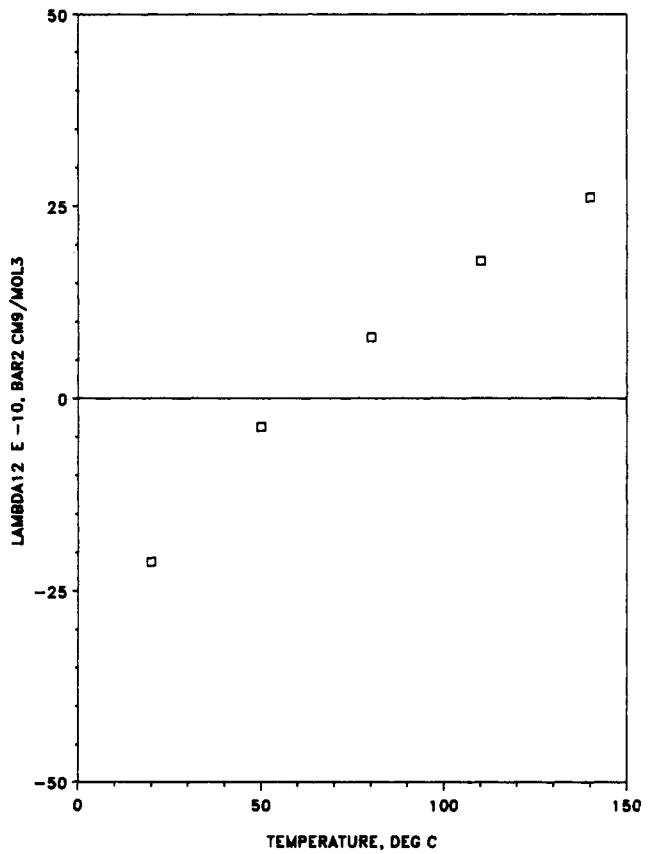

Figure 3. Values of λ_{12} versus temperature.

were used simultaneously with about the same composition, and at the four lowest temperatures, when two pressures are listed for a given overall composition, one is for the increasing temperature part of the cycle and the other is for the decreasing part. That these pressures matched provided evidence that leaks, corrosion, or ammonia decomposition had not occurred. Values of x and y for H_2O, the liquid- and vapor-phase mole fractions that were calculated from eqs 1–6, are also shown in these tables. Liquid volumes from the equation of state sometimes deviated by as much as 10% from experimental values in ref 1. Thus liquid volumes used in eq 1 were calculated not from the equation of state but rather from a correlation that matched these literature liquid volumes to within 2%. Vapor volumes and values of K_i used in eqs 1 and 2 were from the equation of state. Since L, the fraction of moles in the liquid phase, was usually greater than 0.99 and always greater than 0.95, the correction of z_i to x_i as described by eq 2 was small, and thus not sensitive to the parameters in eq 4. This can be seen from Tables IV–VIII by noting that x and z are quite close. Thus, the uncertainty in x is essentially that in z, which is ±0.0004 in mole fraction. Figure 4 shows the experimental and calculated pressures versus composition, and Figure 5 shows deviations between calculated and experimental pressures. Three of the four mixture parameters, k_{ij}^{l}, λ_{12}, and λ_{21}, were set by minimizing the sum of squares of the deviations shown in Figure 5. Also, at each temperature, the points with the lowest ammonia concentration were weighted more heavily so that the deviation between the calculated and experimental pressure for this point was essentially zero. This was done for several reasons. The lowest pressure points were the most accurate, the model does not fit the pressure behavior within experimental uncertainty, and forcing a fit at the

Table VI. Compositions and Experimental Pressures at 353.15 K

z_{H_2O}	x_{H_2O}	y_{H_2O}	P_{exp}, psia
0.9517	0.9522	0.522	12.652
0.9517	0.9522	0.522	12.647
0.9478	0.9485	0.500	13.139
0.9478	0.9485	0.500	13.141
0.9283	0.9292	0.404	15.845
0.9028	0.9039	0.312	19.777
0.9028	0.9039	0.312	19.756
0.8956	0.8970	0.292	21.016
0.8956	0.8970	0.292	20.993
0.8506	0.8522	0.195	29.360
0.8506	0.8522	0.195	29.577
0.8506	0.8522	0.195	29.372
0.8500	0.8520	0.194	29.559
0.8500	0.8520	0.194	29.665
0.8500	0.8520	0.194	29.656
0.8396	0.8415	0.178	31.875
0.8396	0.8415	0.178	32.055
0.8396	0.8415	0.178	32.053
0.8001	0.8022	0.129	41.491
0.8001	0.8022	0.129	41.481
0.7976	0.8000	0.127	42.431
0.7975	0.8002	0.127	42.340
0.7975	0.8002	0.127	42.312
0.6990	0.6998	0.0610	78.385
0.7455	0.7458	0.0844	59.508
0.7455	0.7458	0.0844	59.516
0.6980	0.6985	0.0605	78.766
0.6980	0.6985	0.0605	78.798
0.6014	0.6042	0.0329	131.112
0.6014	0.6042	0.0329	131.314
0.5927	0.5959	0.0313	136.750
0.5927	0.5959	0.0313	136.723
0.5916	0.5948	0.0311	135.965
0.5916	0.5948	0.0311	136.132
0.4985	0.5033	0.0184	204.820
0.4985	0.5033	0.0184	204.580
0.4973	0.5028	0.0184	206.243
0.4973	0.5028	0.0184	205.804
0.2992	0.3096	0.00742	367.860
0.2972	0.3089	0.00740	369.466
0.2074	0.2131	0.00499	448.911
0.2074	0.2136	0.00500	449.592

Table VII. Compositions and Experimental Pressures at 383.15 K

z_{H_2O}	x_{H_2O}	y_{H_2O}	P_{exp}, psia
0.9517	0.9528	0.589	33.859
0.9517	0.9528	0.589	33.807
0.9478	0.9492	0.569	35.003
0.9478	0.9492	0.569	35.008
0.9283	0.9301	0.475	40.977
0.9283	0.9301	0.475	41.135
0.9028	0.9050	0.382	49.727
0.9028	0.9050	0.382	49.640
0.8956	0.8984	0.362	52.489
0.8956	0.8984	0.362	52.257
0.8506	0.8538	0.256	70.333
0.8506	0.8538	0.256	70.169
0.8506	0.8538	0.256	70.457
0.8500	0.8540	0.256	70.578
0.8500	0.8540	0.256	71.072
0.8500	0.8540	0.256	70.507
0.8396	0.8434	0.237	75.415
0.8396	0.8434	0.237	75.995
0.8396	0.8434	0.237	75.862
0.8001	0.8043	0.180	95.405
0.8001	0.8043	0.180	95.242
0.7976	0.8022	0.178	97.031
0.7976	0.8022	0.178	96.976
0.7975	0.8027	0.179	96.656
0.7975	0.8027	0.179	96.617
0.7455	0.7461	0.124	132.339
0.6980	0.6990	0.0939	168.502
0.6980	0.6990	0.0939	168.371
0.4985	0.5069	0.0354	383.037
0.4973	0.5070	0.0354	384.921
0.6014	0.6064	0.0568	260.233
0.5927	0.5985	0.0546	269.881
0.5916	0.5974	0.0543	269.052

Table VIII. Compositions and Experimental Pressures at 413.15 K

z_{H_2O}	x_{H_2O}	y_{H_2O}	P_{exp}, psia
0.9517	0.9536	0.655	77.610
0.9478	0.9503	0.638	79.696
0.9283	0.9314	0.549	91.330
0.9028	0.9066	0.457	107.787
0.8956	0.9004	0.437	112.246
0.8506	0.8560	0.325	145.576
0.8500	0.8567	0.326	146.115
0.8396	0.8460	0.305	154.521
0.8001	0.8070	0.241	189.506
0.7976	0.8053	0.238	193.174
0.7975	0.8061	0.239	192.251
0.6980	0.6995	0.133	316.668

lowest pressure point gave the most reliable value of the Henry's constant for NH_3 in water. Figure 6 shows the pressure deviations for 353.15 K (also shown in Figure 5), as well as the difference between experimental pressures of Gillespie et al. (*1*) and those calculated with the model in this work. Observations to be made from Figures 5 and 6 are (1) the scatter of the data in this study is measurably less than that in the Gillespie data, and, (2) although the method used here gave a better fit to the pressure data than other methods that were examined, the model in this study still does not quite fit the pressures within experimental uncertainty.

In order to illustrate the vapor-phase composition predictions, the relative volatility, which is defined by

$$\alpha = \frac{y_{NH_3} x_{H_2O}}{x_{NH_3} y_{H_2O}} \tag{8}$$

was calculated from y values that were obtained from a bubble point calculation for a specified liquid-phase composition. The relative volatility is plotted in Figure 7 versus composition at 353.15 K. In this figure, the points are the *PTxy* data of Gillespie (*1*), and the solid line corresponds to our values in Table VI, which were calculated with the parameters listed in Table III. The dashed line is from parameters that were determined

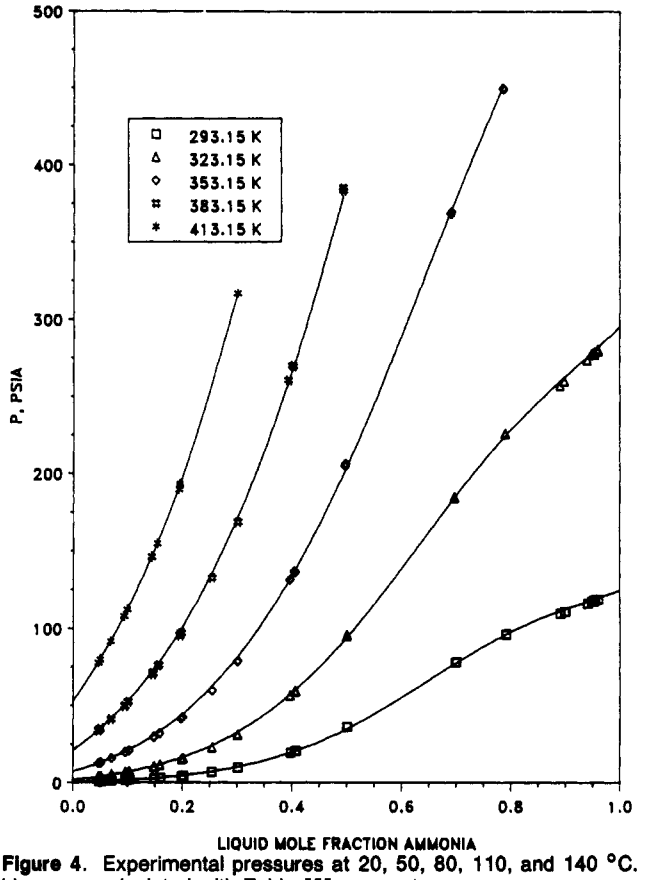

Figure 4. Experimental pressures at 20, 50, 80, 110, and 140 °C. Lines are calculated with Table III parameters.

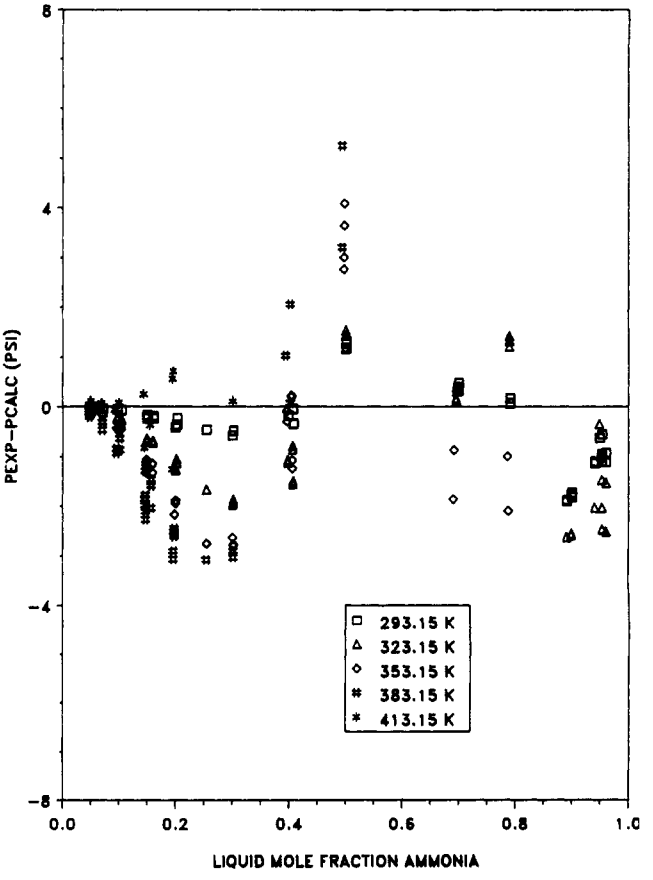

Figure 5. Pressure deviations (experimental minus calculated pressures) (psia).

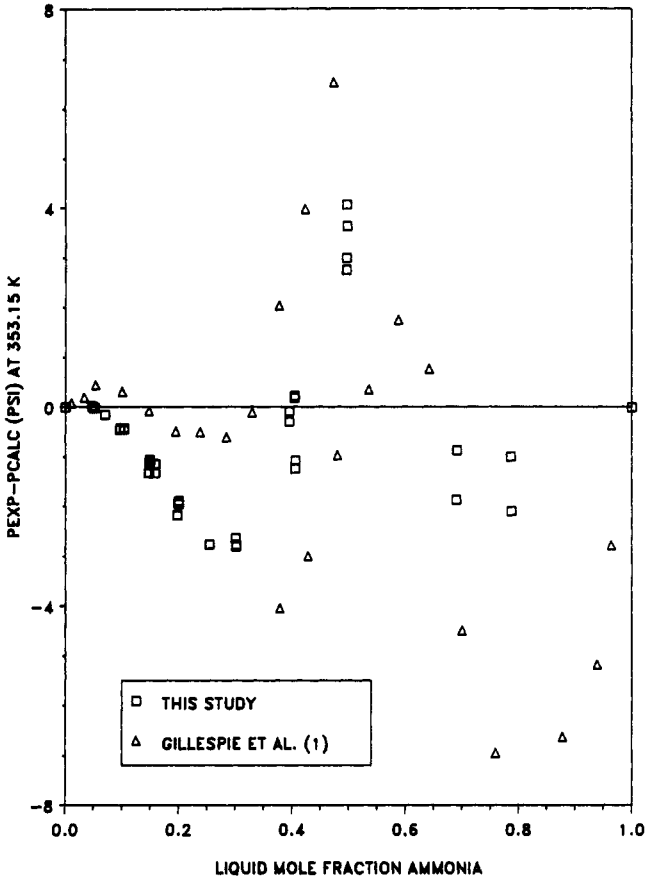

Figure 6. Pressure deviations from this study and for pressures measured by Gillespie et al. (*1*). Points are experimental minus values calculated with Table III parameters.

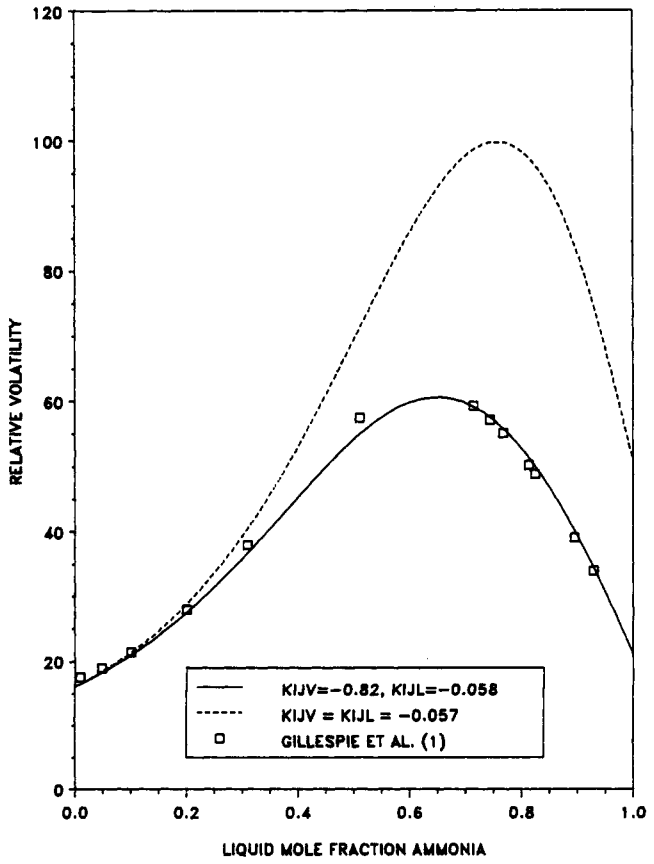

Figure 7. Relative volatility at 80 °C. Points are the data of Gillespie et al. (*1*), solid line is calculated with Table III parameters, and the dashed line is for $k_{ij}^{v} = k_{ij}^{l}$.

Table IX. Henry's Constant for NH_3 in H_2O, psia

	Henry's constant		
T, K	this study	lit. (*22*)	% diff
293.15	10.50	10.95	4.3
323.15	38.5	41.6	8
353.15	110.0	118.2	7
383.15	263.5	271.2	3
413.15	522.3	530.0	1.5

by the same procedure used to generate the Table III parameters (i.e., fit to the pressure data of this study), except that k_{ij} was the same in both phases. Specifically, parameters used to generate the dashed line were $k_{ij} = -0.057$, $\lambda_{12} = 7.83 \times 10^{10}$, and $\lambda_{21} = 27 \times 10^{10}$.

The dashed line in Figure 7 is typical of previous equation-of-state results. Heidemann and Rizvi (*11*) examined eight different equation-of-state variations, and these eight, along with those examined by Ballard and Matherne (*10*), Peng and Robinson (*12*), and Won et al. (*13*), all gave relative volatilities that, at high NH_3 concentrations, were even higher than those given by the dashed line in Figure 7. Only when the vapor-phase k_{ij} was allowed to be different than that in the liquid did the equation of state acquire sufficient flexibility to be able to predict the relative volatilities required by Gillespie's data.

The right half of Figure 7 is for liquid-phase NH_3 mole fractions greater than 0.5 and vapor-phase mole fractions greater than 0.98. Only data from refs 1–5 extend over the entire composition range, and it is these five sets that establish the behavior at high NH_3 concentrations. (The data in refs 6–9, Guillevic et al., Pawlikowski et al. Muller et al., and Sassen et al., either do not extend over the entire composition range or are at temperatures above the critical temperature of NH_3, 405 K, where full range behavior does not exist.) While there are deviations in the data given in refs 1–5, none of these data suggest that the dashed line in Figure 7 represents the true behavior. Gillespie et al. (*1*) claim a repeatability in their α values of 5%, and with this in mind, the estimated uncertainty for the calculated y values in Tables IV–VIII is ±0.005 or ±5%, whichever is smaller.

The quality of the pressure fit for the two curves shown in Figure 7 was essentially the same (average absolute deviation was 1.36 psia). Absolute deviations in y values for the two curves in Figure 7 are also essentially the same, because the vapor is nearly pure ammonia for the right half of Figure 7. If one were not interested in the high ammonia concentration region, any of the traditional equation-of-state methods would be satisfactory. Thus, the main observation is that adjustment of k_{ij}^{v} has essentially no effect on the quality of the pressure fit, but has a dramatic effect on α at high NH_3 concentrations. At low NH_3 concentrations, total pressure data alone are effective in setting the value of α. This can be seen both in Figure 7 (where both curves predict the same value of α at $x_{NH_3} = 0$) and in Table IX, which compares Henry's constants from this study with those calculated from the correlation in ref 23. Values from this study are 1.5–8% lower than the correlation values; Figure 6 indicates that the pressures in this study at low NH_3 concentrations are also about 5% lower than those reported in ref 1.

Using a different k_{ij} value for the liquid and vapor phases is not a completely satisfactory approach. One of the main advantages of the equation-of-state method is that the same model is used to describe both phases, but this advantage is lost when the k_{ij} values are different in the two phases. Also, the highest temperature of this study, 413.15 K, is above the critical temperature of ammonia. With different k_{ij} values in the two phases, the equation of state must necessarily predict incorrect results at a mixture critical point. Nevertheless, adjustment of k_{ij}^{v} does allow the calculation of vapor compositions that are consistent with literature values. The effect of the

rather large negative k_{ij} values that were used for the vapor phase is to make the cross-virial coefficient more negative. Gillespie et al. (*1*) also required large negative cross-virial coefficients in order for their activity coefficient based model to correlate both pressure and vapor-phase behavior. That a single k_{ij} does not accurately describe both the pressure and vapor-phase compositions suggests that the separation of the vapor and liquid phases as expressed by eq 4 is not right. Whether this is because of an incorrect density or composition dependence is not clear, but a worthwhile goal in equation-of-state development would be to modify eq 4 so that the correct behavior would be obtained with a single k_{ij} value. The large negative cross-virial coefficients that are required for the ammonia–water system suggest complex formation that might be better described with some chemical theory. However, introduction of such a model does not alone guarantee success. One of the models examined by Heidemann and Rizvi (*11*) was a reaction-based model, and we have tried to use the reaction-based method of Gmehling et al. (*24*). Neither of these approaches gave satisfactory results.

Conclusions

An accurate $p-x$ data set has been reported for the ammonia–water system for the temperature range of 20–140 °C. An equation-of-state model has been presented and used to generate liquid- and vapor-phase compositions. The liquid compositions are accurate to approximately ±0.0004 in mole fraction. The vapor compositions are accurate to ±0.005 in mole fraction or ±5%, whichever is smaller. The technique of using different values of k_{ij} in the vapor and liquid phases, while not a completely satisfactory approach, did allow the equation-of-state model to reproduce literature relative volatilities at high ammonia concentrations.

Glossary

a,b,c	parameters in eq 3
B	second virial coefficient
k_{ij}^{l}	parameter in eq 4 used for liquid
k_{ij}^{v}	parameter in eq 4 used for vapor
K_i	equilibrium ratio, y_i/x_i
L	fraction of moles in the liquid phase
N_{tot}	total number of moles loaded in cell
P	pressure
R	gas constant
T	temperature
V^l	molar volume of liquid
V^v	molar volume of vapor
V_{cell}	total volume of cell

Greek Letters

α	relative volatitly, see eq 8
λ_{ij}	parameter in eq 4

Literature Cited

(1) Gillespie, P. C.; Wilding, W. V.; Wilson, G. M. In *AIChE Symposium Series 256*; Black, Cline, Ed.; AIChE: New York, 1987; Vol. 83, p 97.
(2) Rizvi, S. S. H.; Heidemann, R. A. *J. Chem. Eng. Data* **1987**, *32*, 183.
(3) Macriss, R. A.; Eakin, B. E.; Ellington, R. T.; Huebler, J. *Physical and Thermodynamic Properties of Ammonia-Water Mixtures*; Research Bulletin No. 34; Institute of Gas Technology: Chicago, IL, 1964.
(4) Wucherer, J. *Z. Gesamte Kaelte-Ind.* **1934**, *41*, 21.
(5) Wilson, T. A., Bulletin No. 146; University of Illinois Engineering Experiment Station: Urbana, IL, 1925.
(6) Guillevic, J. L.; Richon, D.; Renon, H. *J. Chem. Eng. Data* **1985**, *30*, 332.
(7) Pawlikowski, E. M.; Newman, J.; Prausnitz, J. M. *Ind. Eng. Chem. Process Des. Dev.* **1982**, *21*, 764.
(8) Müller, G.; Bender, E.; Maurer, G. *Ber. Bunsen-Ges. Phys. Chem.* **1988**, *92*, 148.
(9) Sassen, C. L.; van Kwartel, R. A. C.; van der Kooi, H. J.; de Swaan Arons, J. *J. Chem. Eng. Data* **1990**, *35*, 140.
(10) Ballard, E. S.; Matherne, J. L. *Chem. Eng. Commun.* **1989**, *84*, 81.
(11) Heidemann, R. A.; Rizvi, S. S. H. *Fluid Phase Equilib.* **1986**, *29*, 439.
(12) Peng, D.-Y.; Robinson, D. B. In *Thermodynamics of Aqueous Systems with Industrial Applications*; Newman, S. A., Ed.; ACS Symposium Series 133; American Chemical Society: Washington, DC, 1980; p 393.
(13) Won, K. W.; Selleck, F. T.; Walker, C. K. Vapor–Liquid Equilibria for the Ammonia-Water System. International Symposium on Phase Equilibria and Fluid Properties in the Chemical Industry, Berlin, Mar 17–21, 1980.
(14) Edwards, T. J.; Newman, J.; Prausnitz, J. M. *Ind. Eng. Chem. Fundam.* **1978**, *17*, 264.
(15) Smolen, T. M. Vapor-Liquid Equilibrium in the Ammonia-Water System. M.S. Thesis, University of Missouri—Rolla, Rolla, MO, 1989.
(16) Fontana, M. G. *Corrosion: A Compilation*; Hollenback Press: Columbus, OH, 1957; p 13. See also: *Ind. Eng. Chem.* **1947** (Sept), *39*, 103A.
(17) Peneloux, A.; Rauzy, E.; Freze, R. *Fluid Phase Equilib.* **1982**, *8*, 7.
(18) Haar, L., and J. S. Gallagher, *J. Phys. Chem. Ref. Data*, *7*, 635, 1978.
(19) Haar, L. *J. Res. Nat. Bur. Stand.* **1968**, *72A*, 207.
(20) Keenan, J. H.; Keyes, F. G.; Hill, P. G.; Moore, J. G. *Steam Tables (S. I. Units)*; Wiley: New York, 1978.
(21) LeFevre, E. J.; Nightingale, M. R.; Rose, J. W. *J. Mech. Eng. Sci.* **1975**, *17*, 243.
(22) Panagiotopoulos, A. Z.; Reid, R. C. *Fluid Phase Equilib.* **1986**, *29*, 525.
(23) Kawazuishi, K.; Prausnitz, J. M. *Ind. Eng. Chem. Res.* **1987**, *26*, 1482.
(24) Gmehling, J.; Liu, D. D.; Prausnitz, J. M. *Chem. Eng. Sci.* **1979**, *34*, 951.

Received for review June 5, 1990. Accepted December 26, 1990. The financial support of the National Science Foundation to carry out this work is gratefully acknowledged.